Molecular Crystals and Liquid Crystals
Publication details, including instructions for authors and subscription information:
http://www.tandfonline.com/loi/gmcl20

Phenoxazine-Based Dyes with Dual Electron Donating Moiety for Organic Dye-Sensitized Solar Cells

Joo Young Kim [a] & Young Sik Kim [a b]

[a] Department of Information Display, Hongik University, Seoul, 121-791, Korea

[b] Department of Science, Hongik University, Seoul, 121-791, Korea

Version of record first published: 18 Oct 2011

To cite this article: Joo Young Kim & Young Sik Kim (2011): Phenoxazine-Based Dyes with Dual Electron Donating Moiety for Organic Dye-Sensitized Solar Cells, Molecular Crystals and Liquid Crystals, 551:1, 138-146

To link to this article: http://dx.doi.org/10.1080/15421406.2011.600633

Mol. Cryst. Liq. Cryst., Vol. 551: pp. 138–146, 2011

ISSN: 1542-1406 print/1563-5287 online
DOI: 10.1080/15421406.2011.600633

Taylor & Francis
Taylor & Francis Group

Phenoxazine-Based Dyes with Dual Electron Donating Moiety for Organic Dye-Sensitized Solar Cells

JOO YOUNG KIM[1] AND YOUNG SIK KIM[1,2,*]

[1]Department of Information Display, Hongik University, Seoul 121-791, Korea
[2]Department of Science, Hongik University, Seoul 121-791, Korea

Highly effective phenoxazine (POZ)–based dyes (dye1, dye2, dye3, dye4 and dye5) for dye-sensitized solar cells (DSSCs) were designed and studied theoretically by using density functional theory (DFT) and time-dependent density functional theory (TDDFT) calculations. When the electronic properties of dye2 were further analyzed in terms of the coupling among its moieties, it was found that the highest occupied molecular orbital (HOMO) and the lowest unoccupied molecular orbital (LUMO) of the dye2 was originated from the HOMO of the POZ and the triphenylamine moieties and the LUMO of the cyanoacrylic acid moiety, respectively. It was found that HOMO = >LUMO (and HOMO-1 = >LUMO) transition could be considered as an intramolecular charge-transfer (ICT) transition and HOMO = >LUMO+1 transition, however, as the mixture of ICT and π–π^* excitation. It was shown that through the additional electron donating group, absorption bands due to HOMO = >LUMO transition were red-shifted and another strong absorption bands appeared as peaks between 400 and 450 nm. Of the POZ-based dyes, we showed that dye5 would have the best photovoltaic properties in terms of light-harvesting efficiency and energy-antenna consideration. These results suggested organic dye sensitizers with dual electron donating group would give good photovoltaic performance for DSSCs.

Keywords dye-sensitized solar cells (DSSCs); phenoxazine (POZ)-based dyes; electron donating group; DFT; TDDFT

Introduction

Dye-sensitized solar cells (DSSCs) have been interested in scientific research and for practical applications due to the potential advantages of low cost, easy production, flexibility, and transparency relative to conventional crystalline silicon solar cells [1, 2]. Performance and stability of DSSC devices have been studied and significantly developed over the past decade [3–5]. Among the components of DSSC, the sensitizer is a crucial element, which significantly influences on the power conversion efficiency as well as the stability of the devices. Up to now, the record for DSSC efficiency was held by a polypyridyl ruthenium sensitizer (11%) in combination with a voltaic iodide/triiodide mixture as electrolyte [6]. However, ruthenium complex dyes are not suitable for the concerns of cost effectiveness and environmental friendliness, because ruthenium is a rare and expensive metal, which limits the potentially wide application of these complexes. Therefore, the investigation of

*Corresponding author. E-mail: youngkim@hongik.ac.kr

DSSCs using metal-free organic dyes has been focused for practical applications [7, 8]. Numerous metal-free organic dyes for DSSCs, such as coumarin- [9], merocyanine- [10], indoline- [11], xanthene- [12], hemicyanine- [13], perylene- [14] and fluorene- [15] based organic dyes, have been developed and showed good DSSC performance.

Recently, it has been reported that metal free organic dyes for DSSCs have a general structure with donor-linker-acceptor [16] and dual donor or dual acceptor group of the dye sensitizers can increase photovoltaic performance [17, 18]. Also, it has been reported that the antenna group of hole transport materials can make charge-recombination process slow through the physical separation of the holes spatially away from the electrons in the semiconductor, and thus improve the efficiency of DSSCs [19, 20].

In this study, phenoxazine (POZ)-based dyes were designed and investigated theoretically by using the density functional theory (DFT) and time-dependent density functional theory (TDDTF) calculations, because of high solar energy-to-electricity conversion efficiency of a POZ-based dye even its simple molecular structure [21]. Specifically, structural, electronic and optical properties of some POZ-based dyes were investigated with the introduction of dual electron donating group. Photovoltaic properties were also investigated in light-harvesting efficiency (LHE) and energy-antenna scheme. Finally, we will suggest high performed dye sensitizer as a DSSC device among the presented POZ-based dyes.

Materials and Methods

A simple POZ dye (dye1) and a POZ-based dye with POZ and triphenylamine (TPA) moieties as dual donating groups (dye2) were selected in this study (see Figure 1). To increase

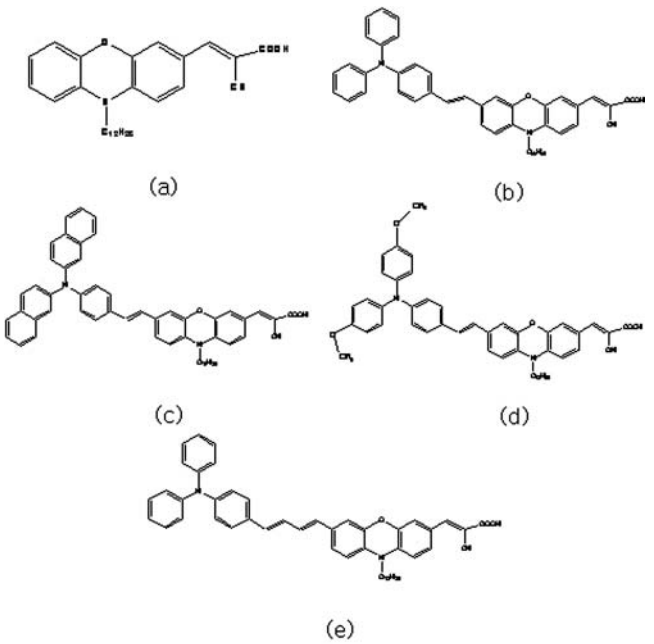

Figure 1. Schematic molecular structures of the POZ-based dyes: (a) dye1 (b) dye2 (c) dye3 (d) dye4 (e) dye5.

absorption efficiency more, other three POZ-based dyes were introduced by modifying from the dye2. The dye3 and the dye4 were designed by adding some TPA-like moieties instead of the TPA moiety. For the dye5, the length of π-conjugation between POZ and TPA moieties was increased, compared to the length of the dye2.

The geometries in the gas phase were optimized by the DFT method using the B3LYP exchange-correlation function with a 6–31G(d) basis set in the Gaussian 03 program package. The lowest energy conformation is found by optimizing the molecular structure of the dyes in the gas phase. Electronic populations of the highest occupied molecular orbital (HOMO) and the lowest unoccupied molecular orbital (LUMO) were calculated to show the position of the localization of electron populations along with the calculated molecular orbital energy diagram.

TDDFT calculations with the B3LYP/6–31G(d) level of theory were performed at the ground-state-optimized geometries. Absorption spectrum was calculated at the ground-state-optimized geometries for some lowest singlet-singlet excitations. The simulation of the absorption spectra was performed by a Gaussian convolution with fwhm = 0.3 eV.

Results and Discussion

DFT calculations were performed at a B3LYP/6–31G level for the geometry optimization of the POZ-based dyes in order to obtain their HOMOs and LUMOs (see Figure 2). For dye1, the electron distribution for the HOMO is mainly localized on the POZ moiety, the LUMO, however, is mainly localized on the cyanoacrylic acid moiety. Through the introduction of electron donating groups with TPA or TPA-like moieties to the dye1, molecular orbitals

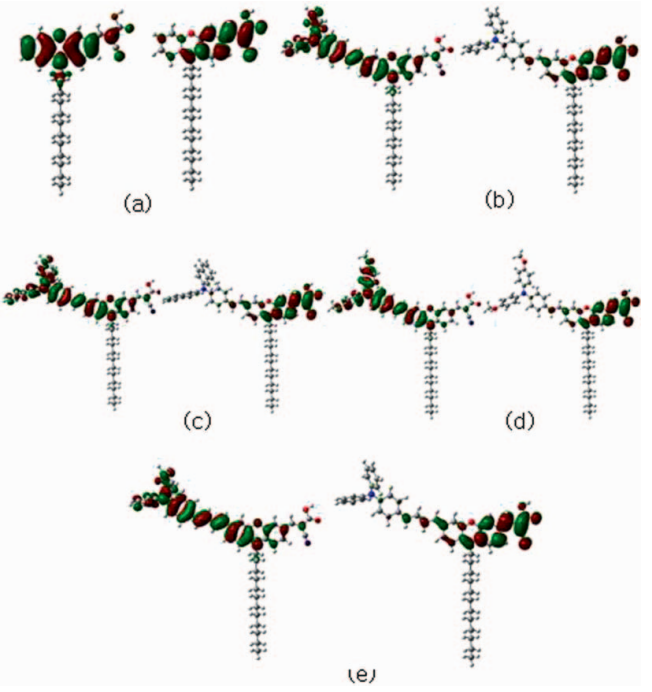

Figure 2. HOMO (left) and LUMO (right) structures of the POZ-based dyes: (a) dye1 (b) dye2 (c) dye3 (d) dye4 (e) dye5.

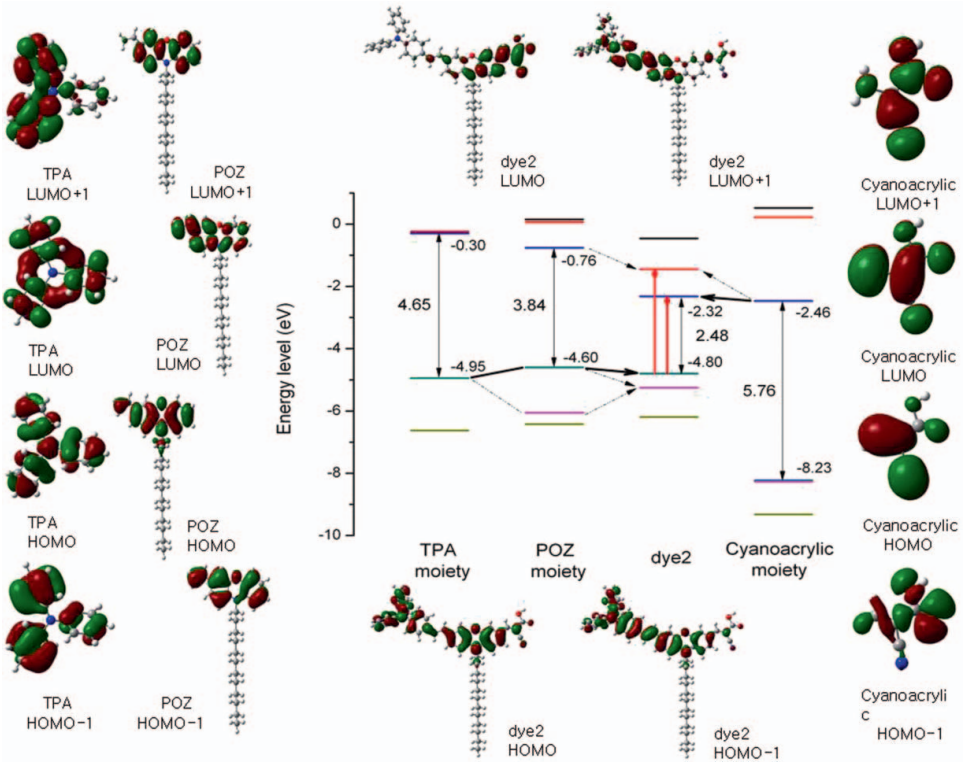

Figure 3. Molecular orbital energy diagram of the dye2, TPA, POZ and cyanoacrylic moieties with their isodensity surface plots of frontier molecular orbitals (MOs). In this figure, thick arrows and line indicate major contributions of the MOs of TPA, POZ and cyanoacrylic moieties to the HOMO and the LUMO of the dye2. Red thick arrows for the dye2 indicate HOMO = >LUMO and HOMO = >LUMO+1 transitions.

(MOs) of the dyes show some different feature. The HOMOs are mainly localized on two electron donating groups, POZ and TPA (TPA-like) moieties for dye2, dye3 and dye4. The HOMO of the dye5 was distributed throughout π-conjugation as well as POZ and TPA moieties. However, the LUMOs of other POZ-based dyes are very similar to that of the dye1, despite of the adding other electron donating groups to the dye1.

It has been reported that retardation in charge-recombination dynamics is related to the physical separation between dye-cation moiety and the surface of the TiO_2 surface [19, 20]. In this study, adding the electron donating group with TPA or TPA-like moiety to the POZ moiety implies the employment of energy antenna group [21]. As shown in Figure 2, the distances between the HOMOs of the dyes and the anchoring moiety slightly changed for different POZ-based dyes and ranged like this: dye1 $<$ dye2 $\sim$ dye3, dye4 $<$ dye5. Therefore, the efficiency of photovoltaic performance would be the same order. This means that after the charge injected from the LUMO to TiO_2, the dye5 would have longer charge-separated lifetime of any other POZ-based dyes in energy-antenna scheme.

In order to investigate the electronic structure of the POZ-based dyes, the dye2 was chosen and analyzed in terms of the coupling among the POZ, the TPA and the cyanoacrylic acid moieties. Figure 3 shows molecular orbital energy diagram of the dye2, the POZ, the TPA and cyanoacrylic moieties with their isodensity surface plots of the frontier MOs. MO

analysis confirmed that the HOMO of the dye2 is delocalized over the POZ and the TPA moieties and has a similar electronic distribution with the HOMOs of the POZ and the TPA moieties. It shows that the HOMO of the dye2 originates in the HOMOs of the POZ and TPA moieties. The LUMO is mainly localized on the cyanoacrylic acid moiety. Although the HOMO−1 of the dye2 has a similar electronic distribution with the HOMO of the dye2, the LUMO+1 has a π-bonding orbital delocalized over the POZ and TPA moieties. Therefore, the HOMO = >LUMO (and the HOMO-1 = >LUMO) transition can be considered as an intramolecular charge-transfer (ICT) transition. This enables that when the dye sensitizer is anchored to TiO_2, the position of the LUMO close to the anchoring group enhances the orbital overlap with the titanium 3d orbitals and favors electron injection. On the other hand, the HOMO = >LUMO+1 transition can be considered the mixture of ICT and π–π^* transition. The electronic origins of the HOMO-1 and the LUMO+1 are also depicted in Figure 3.

TDDFT calculations give insight into the excited states giving rise to the intense absorption bands. In Table 1, we report experimental and computed absorption maxima, oscillator strengths, and major compositions in terms of molecular orbital contributions. We performed these calculations at the B3LYP/6–31G(d) level and for some lowest singlet–singlet excitations (from 5 to 10) up to wavelength of 350 nm. The lowest transition of the dye1 is calculated at 485 nm (2.56 eV) and corresponds to the ICT excitation from the HOMO to the LUMO. When compared to the experimental absorption maximum, found at 491 nm, the calculated transition is in good agreement with the experimental results. For the dye2, the transition calculated at 562 nm is due to HOMO-LUMO transition with ICT. However, the HOMO = >LUMO+1 transition at 406 nm is due to the mixture of ICT and π–π^* excitation. The calculated transitions of the dye2 in terms of molecular orbital energies are also consistent with the experimental results. The good agreements between the experimental and calculated absorption spectra of the dye1 and the dye2 allowed us to investigate further other POZ-based dyes. Excitation properties of other POZ-based dyes were also described in Table 1.

Figure 4 shows the calculated molecular orbital energy diagram for the POZ-based dyes, the TiO_2 nanoparticle model and I^- / I_3^- redox. To consider the molecular levels of the different dyes with the band edges of a model TiO_2 nanoparticle, we use a $Ti_{38}O_{76}$ cluster, and their HOMO and LUMO energies are calculated at −6.55 and −2.77 eV, respectively [6]. The calculated LUMO levels for the dyes are located above the TiO_2 LUMO level. This means that these dye sensitizers have sufficient driving force for electron injection to TiO_2. In addition, HOMO levels of the dye sensitizers are located below the I^- / I_3^- redox, ensuring that there is enough driving force for the dye generation reaction.

As shown in Figure 4, the energy gap between the HOMO and the LUMO of the POZ-based dyes were decreased with the introduction of another electron donating groups or with the increment of π–conjugation length. The energy gap decrement is mainly due to the destabilization of the HOMO levels, since the energy levels of LUMO localized on the cyanoacrylic acid moiety were not nearly changed for the dyes. This could be also predicted from the similarity of LUMOs among the POZ-based dyes from the Figure 2. The reduction of the energy gap of the dye would be represented as a red-shifted energy band in the absorption spectrum. In this respect, the dye4 which contains methoxy moiety shows the most red-shifted energy band and would show higher absorption performance as a photovoltaic device. It is because the electron donating methoxy moiety attached to TPA destabilizes the level of the HOMO and makes the absorption band red-shifted. However, in Table 1, the HOMO = >LUMO+1 transition is another major excitation

Table 1. Major excitation energies and oscillator strengths of the POZ-based dyes (above 350 nm)

Dye	# of excited state	Calculated energy (eV, nm)	Oscillator strength (f)	Major composition	LHE	Transition character	Experimental wavelength[a] (nm)
dye1	1	2.56 (485)	0.3443	Homo => Lumo (82%)	0.547	ICT	491
dye2	1	2.21 (562)	0.6179	Homo => Lumo (89%)	0.759	ICT	517
	2	2.65 (468)	0.1365	Homo-1 => Lumo (85%)	0.270	ICT	
	3	3.06 (406)	0.9177	Homo => Lumo+1 (80%)	0.879	ICT + π =>π^*	390
dye3	1	2.20 (563)	0.6481	Homo => Lumo (89%)	0.775	ICT	
	2	2.61 (475)	0.1612	Homo-1 => Lumo (85%)	0.310	ICT	
	3	2.98 (417)	0.892	Homo => Lumo+1 (81%)	0.872	ICT + π =>π^*	
dye4	1	2.10 (590)	0.4807	Homo => Lumo (92%)	0.669	ICT	
	2	2.54 (488)	0.2729	Homo-1 => Lumo (84%)	0.467	ICT	
	3	3.02 (410)	1.0122	Homo => Lumo+1 (82%)	0.903	ICT + π =>π^*	
dye5	1	2.14 (578)	0.7892	Homo => Lumo (89%)	0.838	ICT	
	2	2.58 (481)	0.2396	Homo-1 => Lumo (80%)	0.424	ICT	
	3	2.85 (435)	1.1002	Homo => Lumo+1 (73%)	0.921	ICT + π =>π^*	

[a] Absorption spectra were measured in CH_2Cl_3 solution at room temperature.

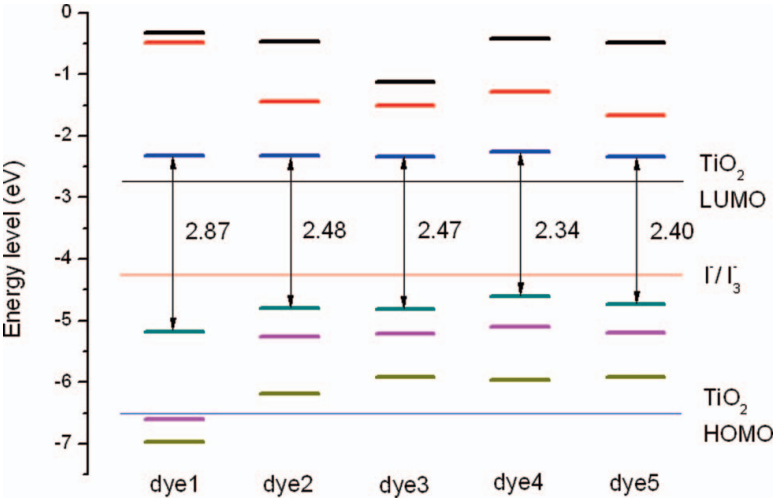

Figure 4. Schematic energy diagram for the POZ-based dyes, a nanocrystalline TiO_2 electrode and I^-/I_3^- redox electrolyte.

because of its larger oscillator strength. Therefore, it is expected that the dye5 would show best photovoltaic performance among the POZ-based dyes.

Figure 5 shows the UV-Vis absorption spectra of the POZ-based dyes by TDDFT calculations. The dye1 has an absorption energy band with a peak at 485 nm, which is ascribed to the HOMO = >LUMO transition and is well consistent with recent result [5]. With the introduction of another electron donating moieties, the HOMO = >LUMO transitions were red-shifted to the absorption bands with peaks at 562, 563, 590, and 578

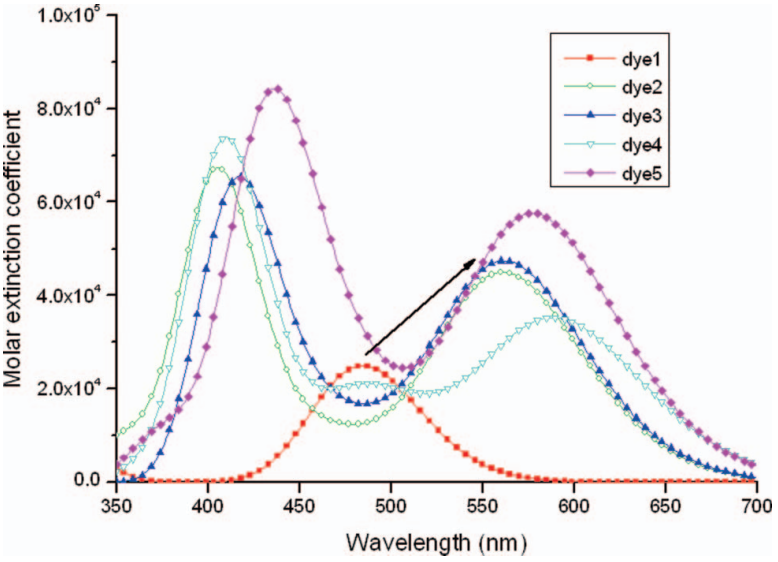

Figure 5. Calculated TDTFT absorption spectra of the POZ-based dyes. The simulation of the absorption spectra has been performed by a Gaussian convolution with fwhm = 0.3 eV.

nm for dye2, dye3, dye4, and dye5, respectively. Another energy bands with peaks between 400 and 450 nm also appeared owing to the additional moieties. These bands were due to HOMO = >LUMO+1 transition, as indicated in Table 1. In general, the POZ-based dyes with dual donating group show better absorbance efficiency compared to the dye1 with the single electron donating group.

Absorption properties as a photovoltaic device can be directly provided in terms of incident photon-to-current conversion efficiency (IPCE) or light-harvesting efficiency (LHE). IPCE and LHE can be expressed as follows:

$$\mathrm{IPCE}(\lambda) = \mathrm{LHE}(\lambda) \cdot \Phi_{\mathrm{inj}} \cdot \eta_{\mathrm{reg}} \cdot \eta_{\mathrm{cc}} \tag{1}$$

$$\mathrm{LHE} = 1 - 10^{-\mathrm{A}} = 1 - 10^{-\mathrm{f}} \tag{2}$$

Where Φ_{inj}, η_{reg}, η_{cc} are the quantum yield of charge injection, dye regeneration and charge collection efficiency, respectively. Although A is the absorbance of the film it can be represented by the oscillator strength (f) in the calculated absorption spectra. If it is assumed that Φ_{inj}, η_{reg}, η_{cc} are all 100% for the dyes, it can be expressed as: IPCE $\sim$ LHE. Table 1 shows calculated LHE converted from the UV-Vis absorption spectra of the POZ-based dyes. LHEs in shorter wavelength region were better than those in longer wavelength region for the dyes with dual donating group. It is suggested that the dye5 would have the best photovoltaic efficiency among the dyes with dual electron donating group.

Conclusions

Some organic POZ-based dyes were designed and studied theoretically as for the potential devices of DSSCs. Specifically, structural, electronic and optical properties of the POZ-based dyes were investigated with the introduction of dual electron donating group. In electronically, although the LUMO levels were not nearly changed, the HOMO levels were changed with the electron distribution throughout two moieties. In the absorption and LHE spectra, the absorption bands due to HOMO = >LUMO transition were red-shifted and another stronger energy bands due to HOMO = >LUMO+1 transition appeared in shorter wavelength region through the additional electron donating moieties. In energy-antenna scheme as well, the POZ-based dyes have a beneficial since HOMOs were distributed throughout the two electron donating moieties, enable to increase physical separation between HOMOs and the anchoring moiety. Overall consideration, it is expected that the dye5 would show the best photovoltaic performance among the POZ-based dye. This study suggests that dual electron donating group should play a crucial role in improving the photovoltaic properties of DSSCs and give insight for developing more efficient organic dyes for DSSCs.

Acknowledgment

This research was supported by Basic Science Research Program through the National Research Foundation of Korea (NRF), funded by the Ministry of Education, Science and Technology (2010-0021668).

References

[1] B. O'Regan, M. Gratzel, *Nature*, **353**, 737, (1991).
[2] M. Gratzel, *Inorg. Chem.*, **44**, 6841, (2005).

[3] D. Kuang, S. Ito, B. Wenger, C. Klein, J. E. Moser, R. Humphry-Baker, S. M. Zakeeruddin, M. Gratzel, *J. Am. Chem. Soc.*, **128**, 4146, (2006).
[4] D. Kuang, C. Klein, S. Ito, J. E. Moser, R. Humphry-Baker, S. M. Zakeeruddin, M. Gratzel, *Adv. Funct. Mater.*, **17**, 154, (2007).
[5] D. Kuang, C. Klein, S. Ito, J. E. Moser, R. Humphry-Baker, N. Evans, F. Duriaux, C. Gratzel, S. M. Zakeeruddin, M. Gratzel, *Adv. Mater.*, **19**, 1133, (2007).
[6] M. K. Nazeeruddin, F. D. Angelis, S. Fantacci, A. Selloni, G. Viscardi, P. Liska, S. Ito, B. Takeru, M. Gratzel, *J. Am. Chem. Soc*., **127**, 16835, (2005).
[7] T. Horiuchi, H. Miura, K. Sumioka, S. Uchida, *J. Am. Chem. Soc.*, **126**, 12218, (2004).
[8] L. Schmidt-Mende, U. Bach, R. Humphry-Baker, T. Horiuchi, H. Miura, S. Ito, S. Uchida, M. Gratzel, *Adv. Mater.*, **17**, 813, (2005).
[9] S. Z. Wang, Y. Cui, K. Hara, Y. Dan-Oh, C. Kasada, A. Shinpo, *Adv. Mater.*, **19**, 1138, (2007).
[10] K. Sayama, K. Hara, N. Mori, M. Satsuki, S. Suga, S. Tsukagochi, Y. Abe, H. Sugihara, H. Arakawa, *Chem. Commun.*, 1173, (2000).
[11] T. Horiuchi, H. Miura, K. Sumioka, S. Uchida, *J. Am. Chem.Soc.*, **126**, 12218, (2004).
[12] K. Hara, T. Horiguchi, T. Kinoshita, K. Sayama, H. Sugihara, H. Arakawa, *Sol. Energy Mater. Sol. Cells*, **64**, 115, (2000).
[13] E. Stathatos, P. Lianos, A. Laschewsky, O. Ouari, P. Van Cleuvenbergen, *Chem. Mater*., **13**, 3888, (2001).
[14] S. Ferrere, A. Zaban, B. J. Gregg, *Phys. Chem. B*, **101**, 4490, (1997).
[15] S. Ferrere, B. Gregg, *New J. Chem*., **26**, 1155 (1997).
[16] T. Marinado, D. P. Hagberg, M. Hedlund, T. Edvinsson, E. M. J. Johansson, G. Boschloo, H. Rensmo, T. Brinck, L. Sun, A. Hagfeldt, *Phys. Chem. Chem. Phys.*, **11**, 133, (2009).
[17] D. P. Hagberg, J. H. Yum, H. Lee, F. D. Angelis, T. Marinado, K. M. Karlsson, R. Humphry-Baker, L. Sun, A. Hagfeldt, M. Gratzel, M. K. Nazeeruddin, *J. Am. Chem. Soc.*, **130**, 6259, (2008).
[18] S. S. Park, Y. S. Won, Y. C. Choi, J. H. Kim, *Energy & Fuels*, **23**, 3732, (2009).
[19] S. A. Haque, S. Handa, K. Peter, E. Palomares, M. Thelakkat, J. R. Durrant, *Angew. Chem., Int. Ed.*, **44**, 5740, (2005).
[20] S. Handa, H. Wietasch, M. Thelakkat, J. R. Durrant, S. A. Haque, *Chem. Commun.*, 1725, (2007).
[21] H. Tian, X. Yang, J. Cong, R. Chen, J. Liu, Y. Hao, A. Hagfeldt, L. Sun, *Chem. Commun.*, 6288, (2009).